RADIATION&APPLICATIONS
ISSN 2466-4294 (online) | rad-journal.org
Vol. 2 | Issue 3 | pp. 175 – 180, 2017
doi: 10.21175/RadJ.2017.03.036
Original research paper

THE ENERGY DEPOSITION DISTRIBUTION AT THE MICRO AND NANO-SCALE FOR MOLECULAR TARGETED RADIOTHERAPY: COMPARISON BETWEEN ^{125}I, ^{99m}Tc AND ^{64}Cu*

S. Di Maria, A. Belchior, Y. Romanets, P. Vaz**

Centro de Ciência e Tecnologias Nucleares, Instituto Superior Técnico,
Campus Tecnológico e Nuclear, Bobadela LRS, Portugal

Abstract. *Given the very short range (micrometers to few nanometers) of Auger electrons (AE), Coster-Kronig (CK) and internal conversion (IC) electrons emitted by several radionuclides, they are nowadays considered as promising solutions for molecular targeted radiotherapy. The aforementioned electrons can locally deposit their energy near the radionuclide decay site, reducing the radiotoxicity of the surrounding healthy tissues in this way. ^{125}I ($T_{1/2}$=59 days, 23 Auger electrons emitted per decay, $\bar{E}_{Auger}$= 520 eV) and ^{99m}Tc ($T_{1/2}$=6 h, 4.4 Auger electrons emitted per decay, $\bar{E}_{Auger}$=213 eV) are two radionuclides that are largely studied for their potential use in theranostic, even if the effectiveness of the ^{99m}Tc Auger emissions in inducing DNA double strand break (DSB) is still controversial. However, in recent years the use of ^{64}Cu ($T_{1/2}$=12.7 h, 1.80 Auger electrons emitted per decay, $\bar{E}_{Auger}$=1134 eV) emerged and became a burning issue, because, in addition to its imaging capabilities, some studies showed that ^{64}Cu has cytotoxicity capabilities when incorporated in radiopharmaceuticals targeted at tumor cells. Therefore, for ^{64}Cu the accurate assessment of the energy deposition pattern near the radionuclide decay site and how this energy varies with the radionuclide-DNA center distance is of paramount importance in order to better design therapeutic strategies based on the Auger electrons emitted by this radionuclide. For this reason, the aim of this work is to study the absorbed dose in the DNA and cell volumes considering the aforementioned three radionuclides described above and for the different spectra emissions of A, CK, IC and β radiation. In order to reach these goals, the state-of-the-art Monte Carlo (MC) radiation transport program MCNP6 was used. For the modeling and simulation purposes, a simplified geometry for the DNA segment, the cytoplasm and the cell, composed of liquid water, was considered and an isotropic-like source was modeled. Emission data (photons were neglected) were obtained from the International Commission on radiological Protection (ICRP) publication ICRP-107. This study shows to what extent the deposited energy pattern distribution is affected when several spectra qualities are considered (Auger, Conversion and β emissions); the discussion and comparison of results (also in terms of S-values calculated in this work and reported by MIRD) obtained for ^{64}Cu with those obtained for ^{125}I and ^{99m}Tc are reported.*

Key words: *Molecular targeted radiotherapy, Auger electrons, energy deposition, Monte Carlo simulations, micro-nano scale modeling*

1. INTRODUCTION

The major interest in radiation therapy is killing tumor cells without affecting the healthy tissue surrounding the tumor.

A great advantage of molecular targeted radiotherapy, with respect to external radiotherapy, is the selectivity of the tumor region, due to new target-specific approaches. The complexity of these new approaches includes multidisciplinary studies of chemical, biological and physical nature. Firstly, it is important to check the availability of radionuclides with specific physical characteristics [1]. The second challenge is to identify radio conjugates able to selectively transport radionuclides to the tumor cells. Finally, the way and the topology of how the radionuclide is attached to the tumor cell is of paramount importance since this characteristic, depending on the type of radiation used (β, α, electrons), could maximize the biological effectiveness for a given tumor type while minimizing crossfire effects. DNA is the primary target for cell inactivation by ionization radiation, since cell death could arise by the lack of repair of complex lesions to DNA [2]. Therefore, in the last decade, there is an increased interest in the use of radionuclides able to emit short-range particles that can generate double strand breaks (DSB) or multiple strand breaks (MSB) at nano level. Auger-electron radionuclide emitters are considered appealing with respect to β emitters, given their shorter range in biological tissues. Even if α-emitters have the potential for molecular targeted radiotherapy, Auger electrons could have a reduced crossfire effect, given the extremely localized energy deposition [3]. Several Auger-emitter radionuclides have been studied and proposed for molecular targeted radiotherapy [3]. Among the Auger-emitter radionuclides, ^{125}I is of particular interest, as it emits about 23 electrons per decay. ^{99m}Tc only emits about 4 electrons per decay, but presents some attractive characteristics, i.e. short half-life, availability and ideal imaging properties for

* The paper was presented at the Fifth International Conference on Radiation and Applications in Various Fields of Research (RAD 2017), Budva, Montenegro, 2017.

** salvatore@ctn.tecnico.ulisboa.pt

therapy monitoring. ^{125}I ($T_{1/2}$=59 days, $\bar{E}_{Auger}$= 520 eV) and ^{99m}Tc ($T_{1/2}$=6 h, $\bar{E}_{Auger}$=213 eV) are two radionuclides that are largely studied for their potential use as theranostic, even if the effectiveness of the ^{99m}Tc Auger emissions in inducing DNA double strand break (DSB) is still controversial [4]. However, in recent years the use of ^{64}Cu ($T_{1/2}$=12.7 h, $\bar{E}_{Auger}$=1134 eV) emerged and became a burning issue, because, in addition to its imaging capabilities, some studies showed cytotoxicity capabilities when associated to radiolabeled compounds in tumor cells [5]. In particular, ^{64}Cu can be employed in the development of theranostics agents by taking advantage of the simultaneous emission of both β^+ and β^- particles for PET imaging and therapy respectively [5]. However, the therapeutic potential of this radionuclide is further enhanced by the decay fraction occurring through electron capture (EC) which stimulates the emission of Auger electrons (1.80 Auger electrons per decay) [6]. The aim of this work was to study the absorbed dose in the DNA and cell volumes considering the aforementioned three radionuclides and for the different emission spectra of Auger electrons (AE), Coster-Kronig (CK), internal conversion (IC) and β radiation.

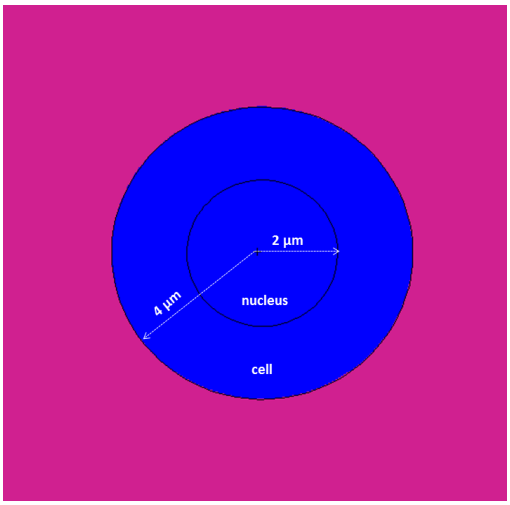

Figure 1. Cell model used for absorbed dose calculations (at micro scale). At the center of the nucleus the nucleosome and DNA volume were also modeled (see Figure 2).

2. Materials and methods

2.1. Monte Carlo simulations

The state-of-art MC simulation program MCNP6 [7] was used in order to calculate the absorbed doses in the volumes of interest. Considering the electron transport, the ENDF/B VI.8 database contains cross sections for the atomic excitation, electron elastic scattering, subshell electro-ionization and bremsstrahlung and is able to simulate electron energies down to 10 eV [8]. In this MCNP6 MC Code version, a completely different approach than that used for higher energies with the condensed-history method was introduced for the transport of energies below 1 keV, that is, single-event electron transport [8], making it a more suitable MC code for micro and nano-dosimetric calculations. MC simulations were used to calculate the absorbed doses in micro and nano volumes. In this type of simulations only the physical stage (space-time distribution of ionization excitations and elastic scattering between the first 10^{-15} s and 10^{-13} s of interaction) was taken into account. Pre-chemical and chemical stages (diffusion and the interaction of water radicals and molecular products) are not considered [9]. The source was simulated as an isotropic source for the ^{64}Cu, ^{125}I and ^{99m}Tc radionuclides. The contributions of radiation considered in this work are reported in Table 1. In particular, IC and β radiation were not taken into account for ^{64}Cu and ^{99m}Tc respectively, because of their negligible yields [10]. The ICRP-107 Auger, IC and β (in this study only the β^- contribution was taken into account) spectra were used for this study [6].

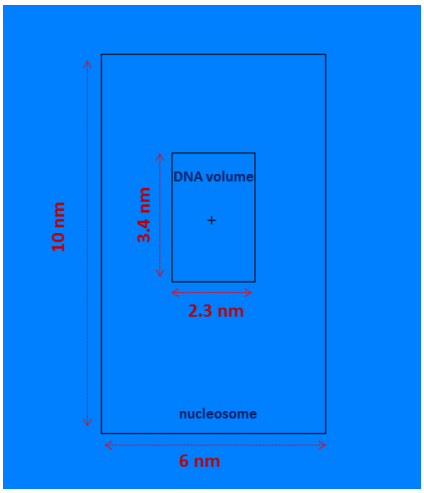

Figure 2. Nucleosome and DNA volume design used for absorbed dose calculations at nano scale

2.2. S-value calculations

The Medical Internal Radiation Dose (MIRD) committee of the American Nuclear Society of Nuclear Medicine [11] made the first attempt to provide dosimetric data at the subcellular level, by using a semi-analytical method (based on the continuous-slowing-down approximation) to calculate the fraction of energy released from the source that is absorbed in the target zone (S-value). MC simulations are considered as the most reliable method for estimating the energy deposition in complex geometries [12].

In order to validate our MC results, the mean absorbed doses in target volumes starting from source volumes (S-values) were calculated according to the MIRD formalism (the model and radii considered are shown in Figure 1). In particular, the general formalism to calculate S-values was [3]:

$$S(T \leftarrow S) = \frac{1}{m_T} \sum_j y_j E_j \emptyset_j (T \leftarrow S)$$

where S and T refer to Source and Target regions, y_j is the electron yield emitted per decay with energy E_j, and

Φ_j (T←S) is the fraction of the source energy deposited in the target region with mass m_T.

Since the calculations involved in this study were focused on a dosimetric estimation inside the nucleus, only the option Target: nucleus and Source: nucleus (N←N) was considered.

More details about S-values calculations and formalism can be found in references [3] and [13].

2.3. Geometry setup for MC calculations

The geometry setups for this work were implemented at micro and at nano scale, according to the different calculations:

a) Micro scale: the geometry was implemented in order to calculate the S-values, according to the MIRD formalism [11] (see Figure 1). Both nucleus and cell were modeled as liquid water;

b) Nano scale: absorbed doses were calculated in a volume corresponding to the DNA segment of 10 base pairs length and a nucleosome, both modeled as liquid water cylinders with nanometric dimensions [14]. Liquid water is the main constituent of the human body and represents a good approximation for the soft biological tissue [15].

Figure 2 illustrates the geometrical setup of the MC simulations performed with the MCNP6 code. The DNA segment was modeled as a water cylinder of 2.3 nm diameter and 3.4 nm heights. This cylinder was set inside another water cylinder with 6 nm diameter and 10 nm height, which represents the nucleosome.

The axes of the DNA segment and nucleosome were aligned along the *z*-axis (height of the DNA cylinder, as shown in Figure 2). The setup of Figure 2 was replicated two times, into two different cell volumes with a radius of 4 μm each. Considering the Figure 3, the isotropic radionuclide source was placed only in the cell A and at 1.08 nm from the central DNA axis. The choice of this distance between the radionuclide and DNA center axis was selected according to some typical values of radionuclide-DNA distances encountered in works where radiolabeled compounds for DNA-targeted Auger therapy are used [4,16]. In fact, in this case, the closer proximity of the radionuclide to the DNA molecule is of paramount importance in order to take advantage of the Auger therapy characteristics. The results in Table 3 are given according to the nomenclature cell A and cell B, where cell A contains the radionuclide source. The MC simulations were quite time-consuming and, for this reason, the number of simulated particles was chosen in order to have a statistical uncertainty of less than 3% for the S-value calculations. However, for the calculations involving nano and micro scales, the statistical uncertainty was less than 8% for the DNA segment, the nucleosome of cell A and cell A, whereas for cell B, the uncertainty reached higher values (of the order of 60%), given the energies and distances involved.

Table 1. Yield values [ICRP-107] considered in this study for ^{125}I, ^{64}Cu, ^{99m}Tc and used for MC simulations

radionuclide	β	IC electron	Auger electron
^{125}I	-	0.94	23.01
^{64}Cu	0.39	5.77E-7	1.80
^{99m}Tc	3.7E-5	1.10	4.41

3. RESULTS AND DISCUSSIONS

3.1. S-values results

One of the main problems for MC simulation validations at micro and nano scale is the lack of experimental data [12]. For this reason, several studies often use MIRD values for comparison with MC calculated values.

In this work, S-values were calculated for a cell and nucleus size of 4 μm and 2 μm, respectively. The results, shown in Table 2, were reported for the self-absorption (N←N) configuration. However, for the sake of comparison, the MIRD values are also reported. In order to compare our results with the MIRD values, the effect of photons was not taken into account in the S-value estimation. The self-absorption S-values calculated with MCNP6 are in good agreement with the MIRD ones for ^{125}I and ^{99m}Tc, since the differences are less than 3%. For ^{64}Cu the difference with the MIRD value reaches about 12%.

The statistical uncertainty reached for the three configurations considered, was less than 3%. The differences between the calculated and MIRD values could be attributed to different calculation approaches: in MIRD electrons propagate in straight trajectories, whereas MCNP6 also takes into account the straggling energy losses [3]. Moreover, the MIRD spectra could be different from the ICRP-107 ones.

Table 2. S values results for ^{125}I, ^{64}Cu and ^{99m}Tc. For comparison, also the MIRD values are reported.

radioisotope	*S-values (Gy/Bq·s) (this work)*	*S-values (Gy/Bq·s) (MIRD)*
	(N←N)	*(N←N)*
^{125}I	4.87E-2 (1.5%)	4.85E-2
^{64}Cu	1.07E-2 (2.8%)	9.33E-3
^{99m}Tc	1.16E-2 (1.5%)	1.19E-2

Table 3. Calculated absorbed doses for ^{125}I, ^{64}Cu and ^{99m}Tc in the volumes of interest.
For each absorbed dose value the relative statistical error is also reported (in parenthesis)

Radiation	***Location***	***Absorbed dose (Gy/Bq·s)***		
		^{125}I	**^{64}Cu**	**^{99m}Tc**
Auger	DNA segment	4.60E6 (1.2%)	3.91E5 (1.1%)	1.39E6 (1.3%)
	Nucleosome (Cell A)	3.34E5 (2.4%)	2.73E4 (1.9%)	1.10E5 (1.3%)
	Cell A	4.41E-3 (3.1%)	1.19E-3 (1.9%)	2.85E-4 (7.7%)
	Cell B	5.33E-5 (60.8%)	-	6.22E-6 (68%)
B$^-$	DNA segment	-	4.43E4 (2.9%)	-
	Nucleosome (Cell A)	-	6.00E3 (2.7%)	-
	Cell A	-	6.61E-4 (1.2%)	-
	Cell B	-	2.07E-5 (12%)	-
IC	DNA segment	3.29E4 (13%)		7.92E4 (5.4%)
	Nucleosome (Cell A)	5.15E3 (7.4%)		1.21E4 (3.1%)
	Cell A	2.09E-3 (0.3%)		1.14E-3 (0.6%)
	Cell B	5.09E-5 (13%)		8.22E-6 (34%)

3.2. Dose comparison for ^{64}Cu, ^{99m}Tc and ^{125}I

The absorbed doses were calculated for each radionuclide and for each volume reported in Table 3. Considering the absorbed dose, the results derived by the contribution of the Auger source, ^{125}I is able to deliver the highest absorbed dose per decay in all regions studied (DNA segment, Nucleosome of Cell A, Cell A and Cell B), probably due to the highest Auger electron yield for this radionuclide (see Table 1). In particular, the absorbed dose in the DNA segment for ^{125}I is one order greater than the ^{64}Cu and about 70% greater than ^{99m}Tc. This could mean that the ^{125}I could be more effective in inducing DSBs at DNA level. However, looking at a micro scale (cell A in Table 3), the difference between ^{64}Cu and ^{125}I is reduced, since the absorbed dose per decay in the cell containing the ^{64}Cu source is about 70% less than ^{125}I. This issue could indicate that Auger spectrum of ^{64}Cu may be also effective at micro scale, since the energy deposition in the cell is comparable with ^{125}I.

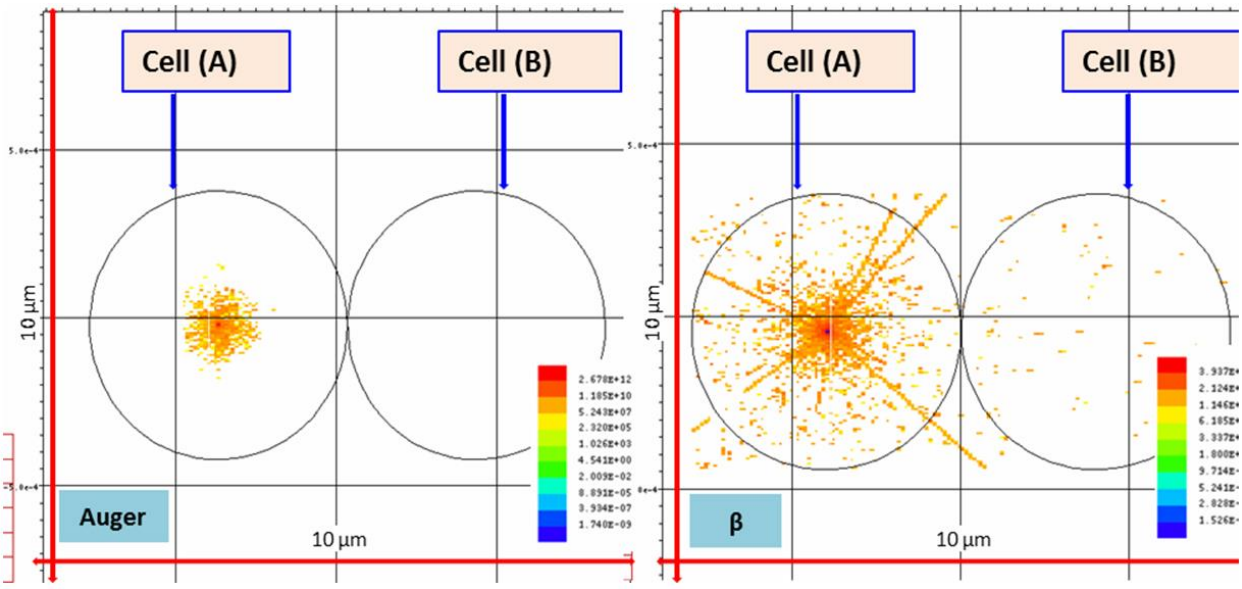

Figure 3. Auger (left) and β$^-$ (right) absorbed dose distributions for ^{64}Cu radionuclide. The dose values of the Mesh tally are in MeV/g/particle units. The emitting source was placed inside the cell A at 1.10 nm from the DNA axis volume (see section 2.3 for further details).

Considering the IC contribution for ^{125}I and ^{99m}Tc and the β$^-$ contribution for ^{64}Cu to the absorbed dose per decay in all four regions considered, the difference between the three radionuclides is less accentuated. For example, the absorbed dose in the DNA segment due to the β$^-$ radiation for ^{64}Cu is greater (about 20%)

than ^{125}I IC contribution. These results then also show how important the inclusion of IC and β^- radiation for dosimetric purposes is. In fact, considering the total absorbed dose in the DNA segment due to the contribution of Auger and β^- radiation for ^{64}Cu, the β radiation represents about 10% of the total absorbed dose in DNA volume.

The statistical uncertainty varies according to the proximity of the source to the scoring volume. As reported in Table 3, statistical uncertainties for DNA, nucleosome of cell A and cell A are less than 8%, for Auger, IC and β radiation. In the case of the cell B volume, the uncertainties reach values of about 60%-70%. In this case, the computational time required to reach better statistics would be prohibitive, even with the cluster computer tools. These large variances are partially due to naturally observed variance in energy deposition due to the stochastic nature of the radiation interactions and the very low observed dose. Nevertheless, considering that all the electron energies used in this study have short ranges in liquid water (of the order of nano to few micro), the contribution for higher distances should be very small. Moreover, even if the uncertainties in the cell B regions are high, their absolute dose values are very small (of the order of 10^{-5}-10^{-6} Gy/decay).

Figure 3 shows the absorbed dose distribution of ^{64}Cu as a source, and the absorbed dose distribution of Auger and β^- contributions. The absorbed dose distribution was calculated through the *mesh tally* function with MCNP6. The images refer to the radial plane x-y, with the z-axis fixed at the source coordinate. The absorbed dose values reported in the images are the tally results expressed in MeV/g/particle units. It is interesting to note how the absorbed dose distribution due to Auger radiation (left image of Figure 3) is all localized in a spherical volume of about 1 μm in radius. On the other hand, given the more penetrating β^- radiation, a greater spread in energy deposition is achieved around the source decay site (right side of Figure 3). In this case, some particle tracks with the higher energy (of the order of 600 keV) are able to cross the entire cellular radius depositing energy in the cell.

4. Conclusions

In this study, a dosimetric assessment at micro and nano scale and for three radionuclides (^{125}I, ^{64}Cu and ^{99m}Tc) was performed. Since ^{125}I is largely studied in literature, it was chosen in order to have the reference values in terms of the absorbed dose for the other two radionuclide considered (^{99m}Tc and ^{64}Cu). In terms of the absorbed dose per decay, ^{125}I is the one that shows the best performance. However, in the choice of the best radionuclide to use for a given targeted radiotherapy purpose, the rationale should also be extended to other factors, such as the availability of the isotope, effective mode of binding with appropriate chemical carrier, half-life and energies of the radionuclide emission [5].

If looking only at the spectral characteristic of the radionuclide, ^{125}I is the better option, as also showed in the results of Table 3. In addition, if also the decay time properties of the radionuclides are taken into account, the potential of ^{64}Cu could be more evident. In fact, the ^{125}I has a half-life time of 1416 *h*, meaning that has a decay probability of about 0.05% per hour, whereas ^{64}Cu and ^{99m}Tc have a decay probability of about 6% and 11% per hour respectively. This means that in a short time interval ^{99m}Tc and ^{64}Cu could deliver more doses to the target of interest with respect to ^{125}I. The dose rate delivered to a target tumor cell is strictly linked with the capability of the radionuclide to induce cell death and with the repair capabilities of the cells, among other factors. It was reported, for example, that a higher dose rate delivered could be beneficial to efficiently killing tumor cells [17, 18]. It is also worth to say that the dose rate in radionuclide therapy is at least two orders of magnitude lower than in external radiotherapy [19]. Nevertheless, the effect of the dose rate on the cellular cytotoxicity is beyond the scope of this study. This study shows that ^{64}Cu, when compared to ^{125}I and ^{99m}Tc have the potential for targeted radiotherapy purposes when the energy distribution pattern caused by Auger emission is taken into account. Finally, even if the IC and β^- yields are smaller than Auger ones, their inclusion in targeted therapy strategies could have a non-negligible impact at micro and nano level and simulation studies should include all radiation emitted by the radionuclide to have a full understanding from the dosimetric point of view.

Acknowledgement: *The authors gratefully acknowledge the Fundação para a Ciência e Tecnologia for supporting this work through the UID/Multi/04349/2013 project and the grant SFRH/BPD/112654/2015.*

References

1. R. W. Howell, "Auger processes in the 21st century," *Int. J. Radiat. Biol.*, vol. 84, no. 12, pp. 959 – 975, Dec. 2008. DOI: 10.1080/09553000802395527 PMid: 19061120 PMCid: PMC3459331
2. P. L. Olive, "The role of DNA Single- and Double Strand Breaks in cell killing by Ionizing Radiation," *Radiat. Res.*, vol. 150, no. 5, pp. S42-S51, Nov. 1998. DOI: 10.2307/3579807 PMid: 9806608
3. N. Falzone, J. M. Fernández-Varea, G. Flux, K. A. Vallis, "Monte Carlo Evaluation of Auger Electron–Emitting Theranostic Radionuclides," *J. Nucl. Med.*, vol. 56, no. 9, pp. 1441 – 1446, Sep. 2015. DOI: 10.2967/jnumed.114.153502 PMid: 26205298
4. P. Balagurumoorthy et al., "Effect of distance between decaying ^{125}I and DNA on Auger electron induced double-strand break yield," *Int. J. Radiat. Biol.*, vol. 88, no. 12, pp. 998 – 1008, Dec. 2012. DOI: 10.3109/09553002.2012.706360 PMid: 22732063 PMCid: PMC3755766
5. A. N. Asabella et al., "The Copper Radioisotopes: A Systematic Review with Special Interest to ^{64}Cu," *BioMed Res. Int.*, vol. 2014, 786463, 2014. DOI: 10.1155/2014/786463
6. K. Eckerman et al., "ICRP Publication 107. Nuclear decay data for dosimetric calculations," *Ann. ICRP*, vol. 38, pp. 7 – 96, 2008.

PMid: 19285593
7. T. Goorley et al., "Initial MCNP6 release overview MCNP6 version 1.0," Los Alamos National Laboratory, Los Alamos (NM), USA, Rep. LA-UR-13-22934, 2013. Retrieved from: http://permalink.lanl.gov/object/tr?what=info:lanl-repo/lareport/LA-UR-13-22934 Retrieved on: Aug. 7, 2017
8. G. Hughes, "Recent developments in low-energy electron/photon transport for MCNP6," *Prog. Nuc. Sci. Tech.*, vol. 4, pp. 454 – 458, 2014. DOI: 10.15669/pnst.4.454
9. H. Nikjoo et al., "Track-structure codes in radiation research," *Radiat. Meas.*, vol. 41, no. 9-10, pp. 1052 – 1074, Oct-Nov. 2006. DOI: 10.1016/j.radmeas.2006.02.001
10. C. Champion et al., "Comparison between Three Promising ß-emitting Radionuclides, ^{67}Cu, ^{47}Sc and ^{161}Tb, with Emphasis on Doses Delivered to Minimal Residual Disease," *Theranostics*, vol. 6, no. 10, 2016. DOI: 10.7150/thno.15132 PMid: 27446495 PMCid: PMC4955060
11. S. M. Goddu, *MIRD Cellular S-values*, Reston (VA), USA: Society of Nuclear Medicine, 1997.
12. M. A. Tajik-Mansoury, H. Rajabi and H. Mazdarani, "A comparison between track-structure, condensed-history Monte Carlo simulations and MIRD cellular S-values," *Phys. Med. Biol.*, vol. 62, no. 5, pp. N90 – N106, Mar. 2017. DOI: 10.1088/1361-6560/62/5/N90 PMid: 28181480
13. A. Taborda et al., "Dosimetry at the sub-cellular scale of Auger-electron emitter ^{99m}Tc in a mouse single thyroid follicle," *Appl. Radiat. Isot.*, vol. 108, pp. 58 – 63, Feb. 2016. DOI: 10.1016/j.apradiso.2015.12.010 PMid: 26704702
14. P. Lazakaris et al., "Comparison of nanodosimetric parameters of track structure calculated by the Monte Carlo codes Geant4-DNA and PTra," *Phys. Med. Biol.*, vol. 57, no. 5, pp. 1231 – 1250, Mar. 2012. DOI: 10.1088/0031-9155/57/5/1231 PMid: 22330641
15. M. Dingfelder et al., "Comparisons of Calculations with PARTRAC and NOREC: Transport of Electrons in Liquid Water," *Radiat. Res.*, vol. 169, no. 5, pp. 584 – 594, May 2008. DOI: 10.1667/RR1099.1 PMid: 18439039 PMCid: PMC3835724
16. E. Pereira et al., "Evaluation of Acridine Orange Derivatives as DNA-Targeted Radiopharmaceuticals for Auger Therapy: Influence of the Radionuclide and Distance to DNA," *Sci. Rep.*, vol. 7, 42544, Feb. 2017. DOI: 10.1038/srep42544
17. L. Jiang et al., "*In vitro* and *in vivo* studies on radiobiological effects of prolonged fraction delivery time in A549 cells," *J. Radiat. Res.*, vol. 54, no. 2, pp. 230 – 234, Mar. 2013. DOI: 10.1093/jrr/rrs093 PMid: 23090953 PMCid: PMC3589931
18. J. F. Fowler et al., "Loss of biological effect in prolonged fraction delivery," *Int. J. Radiat. Oncol. Biol. Phys.*, vol. 59, no. 1, pp. 242 – 249, 2004. DOI: 10.1016/j.ijrobp.2004.01.004 PMid: 15093921
19. J. Carlsson et al., "Requirements regarding dose rate and exposure time for killing of tumour cells in beta particle radionuclide therapy," *Eur. J. Nucl. Med. Mol. Imaging*, vol. 33, no. 10, pp. 1185 – 1195, Oct. 2006. DOI: 10.1007/s00259-006-0109-3 PMid: 16718515 PMCid: PMC1998878